© 2019. Published by The Company of Biologists Ltd | Journal of Cell Science (2019) 132, jcs224097. doi:10.1242/jcs.224097

RESEARCH ARTICLE

The connexin 30 A88V mutant reduces cochlear gap junction expression and confers long-term protection against hearing loss

John J. Kelly, Julia M. Abitbol, Stephanie Hulme, Eric R. Press, Dale W. Laird* and Brian L. Allman*,‡

ABSTRACT

Mutations in the genes that encode the gap junction proteins connexin 26 (Cx26, encoded by *GJB2*) and Cx30 (*GJB6*) are the leading cause of hereditary hearing loss. That said, the Cx30 p.Ala88Val (A88V) mutant causes Clouston syndrome, but not hearing loss. Here, we report that the Cx30-A88V mutant, despite being toxic to inner ear-derived HEI-OC1 cells, conferred remarkable long-term protection against age-related high frequency hearing loss in $Cx30^{A88V/A88V}$ mice. During early development, there were no overt structural differences in the cochlea between genotypes, including a normal complement of hair cells; however, the supporting cell Cx30 gap junction plaques in mutant mice were reduced in size. In adulthood, $Cx30^{A88V/A88V}$ mutant mice had a reduction of cochlear Cx30 mRNA and protein, yet a full complement of hair cells. Conversely, the age-related high frequency hearing loss in $Cx30^{+/+}$ and $Cx30^{+/A88V}$ mice was due to extensive loss of outer hair cells. Our data suggest that the Cx30-A88V mutant confers long-term hearing protection and prevention of hair cell death, possibly via a feedback mechanism that leads to the reduction of total Cx30 gap junction expression in the cochlea.

KEY WORDS: Connexin, Gap junction, Hearing, Mouse, Cx30, GJB6, Clouston syndrome, Aging

INTRODUCTION

Connexins (Cxs) are a large family (21 subtypes in humans) of transmembrane proteins that oligomerize into hexameric structures known as connexons. When trafficked to the cell surface, connexons can function independently as 'hemichannels' or dock with a compatible connexon on an adjacent cell to form direct cell–cell communication channels called gap junctions (Laird, 2006; Sáez and Leybaert, 2014). The Cx composition of gap junctions helps regulate and direct the movement of ions and small metabolites (Alexander and Goldberg, 2003; Neijssen et al., 2005) between cells, or in the case of hemichannels, between cells and the external milieu (Anselmi et al., 2008). Therefore, gap junctions and hemichannels are proposed to have roles in several processes such as cell signalling, tissue development, potassium buffering and intercellular biochemical coupling for coordination of tissue responses such as wound healing, to name just a few. It is now apparent that almost all tissues in the human body require some degree of gap junctional intercellular communication (GJIC), as evidenced by over two dozen distinct diseases associated with connexin gene mutations (Kelly et al., 2015). GJIC is aided by the accumulation of hundreds to thousands of gap junction channels into large plaque-like regions between cells. In particular, the non-sensory cells of the cochlea express some of the largest gap junction plaques in mammals and are extensively coupled by two gap junction networks, the epithelial and connective tissue gap junction networks (Forge et al., 2003b; Kikuchi et al., 1995). Connexin 26 (Cx26, encoded by *GJB2*) and Cx30 (*GJB6*) are the main Cx subtypes found within both gap junction networks of the cochlea where they can assemble into mixed heteromeric or heterotypic channels (Ahmad et al., 2003; Forge et al., 2003a; Lautermann et al., 1998). The importance of Cx26 and Cx30 to hearing and cochlear homeostasis is highlighted by the fact that mutations in the genes that encode Cx26 (*GJB2*) and Cx30 (*GJB6*) in humans are the most common cause of inherited non-syndromic pre-lingual deafness (Chan and Chang, 2014; Kenneson et al., 2002; Snoeckx et al., 2005). In these instances, hearing loss is the only phenotypic outcome of the mutation; however, other tissues also express Cx26 and Cx30, such as the skin and glial networks in the brain. Depending on the type of mutation in the *GJB2* or *GJB6* genes, other comorbidities such as skin disease may (syndromic) or may not (non-syndromic) occur with hearing loss, such as the rare autosomal dominant disorder Clouston syndrome (OMIM #129500).

Clouston syndrome, also known as hidrotic ectodermal dysplasia, is characterized by thin, wiry hair, alopecia, thickening and hyperpigmentation of the skin and dystrophy of the nails (Fraser and Der Kaloustian, 2001; Lamartine et al., 2000). Currently, at least four missense mutations causing amino acid substitutions G11R, V37E, D50N and A88V in the Cx30 polypeptide chain are associated with Clouston syndrome (Baris et al., 2008; Chen et al., 2010; Jan et al., 2004; Smith et al., 2002; Zhang et al., 2003). In most instances, hearing loss is not associated with Clouston syndrome, and only appears in patients with double heterozygosity for mutations in both the Cx26 and Cx30 genes (Jan et al., 2004; Sugiura et al., 2013). This preservation of hearing in Clouston syndrome patients harbouring only the *GJB6* mutation encoding Cx30-A88V is intriguing given that our previous *in vitro* studies found that expressing the Cx30-A88V mutant alone in both HeLa cells and rat epidermal keratinocytes (REK cells) induced potent activation of cleaved caspase 3 and consequent cell death (Berger et al., 2014). Based on these results, we postulated that the Cx30-A88V mutant leads to a loss of channel control and 'leaky' hemichannels either from within intracellular compartments or at the cell surface, the latter of which has also been reported by others (Essenfelder et al., 2004). Although these *in vitro* studies showed that the Cx30-A88V mutant can be highly toxic when overexpressed in certain cell lines, it is unclear if this toxicity is cell-type specific, raising the possibility that cochlear cells are more resistant to the effects of the Cx30-A88V mutant.

Department of Anatomy and Cell Biology, University of Western Ontario, London, Ontario N6A 5C1, Canada.
*These authors contributed equally to this work

‡Author for correspondence (brian.allman@schulich.uwo.ca)

B.L.A., 0000-0001-8793-2019

Received 17 August 2018; Accepted 6 December 2018

Journal of Cell Science (2019) 132, jcs224097. doi:10.1242/jcs.224097

To elucidate the mechanisms by which the Cx30-A88V mutant causes Clouston syndrome, Bosen and colleagues created a mouse model of the disease on a CD-1 mouse background (Bosen et al., 2014). These Cx30-A88V mutant mice exhibited hyperproliferative and enlarged sebaceous glands, and mild palmoplantar hyperkeratosis (Bosen et al., 2014), as well as an unusual hearing profile compared to wild-type mice that was characterized by poorer (elevated) hearing thresholds within the lower frequency ranges in the apical region of the cochlea (<10 kHz), but substantially improved hearing within the high frequency, basal region of the cochlea (Bosen et al., 2014; Lukashkina et al., 2017). This hearing profile is particularly interesting given that CD-1 mice usually suffer from an inherent early-onset, progressive hearing loss (Mahendrasingam et al., 2011). At present, however, it remains unknown whether the Cx30-A88V mutant confers long-term protection to high frequency hearing during aging, because the aforementioned studies on Cx30-A88V mutants were restricted to assessing young adult mice between 3 and 9 weeks of age (Bosen et al., 2014; Lukashkina et al., 2017). Moreover, although the skin of Cx30-A88V mutant mice showed similar Cx30 expression levels to that of wild-type mice (Bosen et al., 2014), no prior studies have investigated whether the expression levels of Cx30 – and possible influence on Cx26 – differ in the cochleae of mutant mice, or how the Cx30-A88V mutant affects the sensorineural and supporting cells during aging.

In the present study, we used a combination of *in vitro* and *in vivo* techniques to determine the effect of the Cx30-A88V mutant on age-related changes in the structure and function of the mouse cochlea. First, to investigate the potential for cell-specific toxicity caused by the Cx30-A88V mutant, we overexpressed it in an inner ear cell line (House Ear Institute-Organ of Corti, HEI-OC1 cells) derived from the Immortomouse (Kalinec et al., 2016) that would normally express Cx30 *in vivo*. Next, we harvested the cochleae from neonatal mutant and wild-type mice, and prepared organotypic cultures that were immunolabelled to reveal Cx30-A88V mutant-related changes in gap junction morphology, including Cx30 plaque density and size. Ultimately, to determine whether the unusual hearing profile previously reported in Cx30-A88V mutant mice (Bosen et al., 2014; Lukashkina et al., 2017) exhibited long-term protection against hearing loss, we assessed the hearing thresholds in the mutant versus wild-type mice at both 3 and 6 months of age. At these same aging time points, adult mice were euthanized and cochlear cryosections were immunolabelled to assess the gross morphology and gene expression profile of the cochlear lateral wall. Finally, to determine whether the Cx30-A88V mutant protected against the age-related death of sensorineural cells in mice on the CD-1 background, we immunolabelled cochlear cryosections and whole mounts of 3- and 6-month-old Cx30-A88V mutant and wild-type mice for markers of sensory hair cells and spiral ganglion neurons. Taken together, the results of this study provide an improved understanding of the important and complex role Cx30 plays in the structure and function of cochlear cells across the lifespan.

RESULTS

The Cx30-A88V mutant is cytotoxic to HEI-OC1 cells

Our lab and others have shown that the Cx30-A88V mutant is cytotoxic when overexpressed in HeLa and REK cell lines, and that co-expression of Cx26 is unable to rescue this effect (Berger et al., 2014; Essenfelder et al., 2004; Lu et al., 2018). To determine whether cochlear cells, which would normally express Cx30 *in vivo*, are particularly resistant to the cytotoxic effects of the mutant, Cx30 (wild-type) and Cx30-A88V, in addition to C-terminal GFP-tagged variants, were overexpressed in an inner ear cell line (HEI-OC1). Cells expressing Cx30 or Cx30–GFP appeared healthy and formed normal gap junction plaques between Cx30-expressing cells (Fig. 1). However, in a similar fashion to our previous *in vitro* studies (Berger et al., 2014), both the untagged and GFP-tagged Cx30-A88V mutants were cytotoxic, as evidenced by pyknotic nuclei and a shrunken cytoplasm (Fig. 1). There was also a distinct lack of gap junction plaques between cells expressing mutant Cx30-A88V, indicating that HEI-OC1 cells are also susceptible to Cx30-A88V-induced cytotoxicity, as seen previously in HeLa, REK and HaCaT cells (Berger et al., 2014; Essenfelder et al., 2004; Lu et al., 2018). To further elucidate the subcellular localization of the Cx30-A88V mutant in the limited number of cells that survived, we immunostained for markers of intracellular compartments and found that a substantial amount of Cx30-A88V co-localized with GM130, a marker for the Golgi apparatus (Fig. S1).

Cx30-A88V mutant mice exhibit prolonged protection against hearing loss in CD-1 mice

Since the Cx30-A88V mutant was found to be toxic *in vitro*, it was somewhat surprising that a mouse model expressing the mutant did not exhibit pronounced hearing loss (Bosen et al., 2014). In fact, mice expressing the mutant showed better hearing profiles than their wild-type and heterozygote litter mate controls at 6–9 weeks of age (Bosen et al., 2014). In the present study, we sought to extend this finding and determine whether the mutant also confers long-term protection against hearing loss in aging mutant mice by assessing their hearing profiles. To do so, we used the auditory brainstem response (ABR), which is a measure of the electrical activity in the brainstem evoked by the repeated presentation of a given acoustic stimulus. Initially, the hearing profiles of all genotypes in the first week after weaning (3–4 weeks old) showed no significant difference in their ability to detect broadband noise (click stimuli, Fig. 2A). Paradoxically, the hearing thresholds at low frequencies (4 and 8 kHz) were significantly higher in homozygous ($Cx30^{A88V/A88V}$) mice compared to wild-type ($Cx30^{+/+}$) and heterozygous ($Cx30^{+/A88V}$) littermate controls (indicative of worsened hearing in homozygous mutant mice), whereas those at the higher frequencies (24 and 32 kHz) were significantly lower (indicative of better hearing) (Fig. 2A). At 3 months of age, wild-type mice showed progressive high-to-low frequency hearing loss, whereas homozygous mice showed significantly better hearing at the click stimulus and at 16, 24 and 32 kHz (Fig. 2A). Even at 6 months of age, homozygous mice showed significantly better hearing thresholds at the click, 16, 24 and 32 kHz stimuli (Fig. 2A). Interestingly, a comparison of one wild-type and one homozygote mutant mouse at 1 year of age (shown as grey shaded lines in the 6 months graph) revealed extended hearing protection in the homozygote. Owing to a lack of mice at this age, these data represent single mouse ABR profiles and were not used for any statistical analysis.

To assess the neural output transmitted along the auditory nerve exiting the cochlea, we next determined the latency (Fig. 2B, in ms) and amplitude (Fig. 2C, in µV) of the peak of the first wave of the ABR (wave I) in response to the 90 dB sound pressure level (SPL) click stimulus. These measurements give a general indication of the number and integrity of neurons firing (measured by the amplitude) as well as the conduction speed of those neurons (measured by the latency from stimulus onset to wave I) after hair cell activation. Representative ABR traces of the amplitudes and latencies of all three genotypes are shown in Fig. S2. At 3 and 6 months of age, homozygous mutant mice displayed significantly faster wave I

Journal of Cell Science (2019) 132, jcs224097. doi:10.1242/jcs.224097

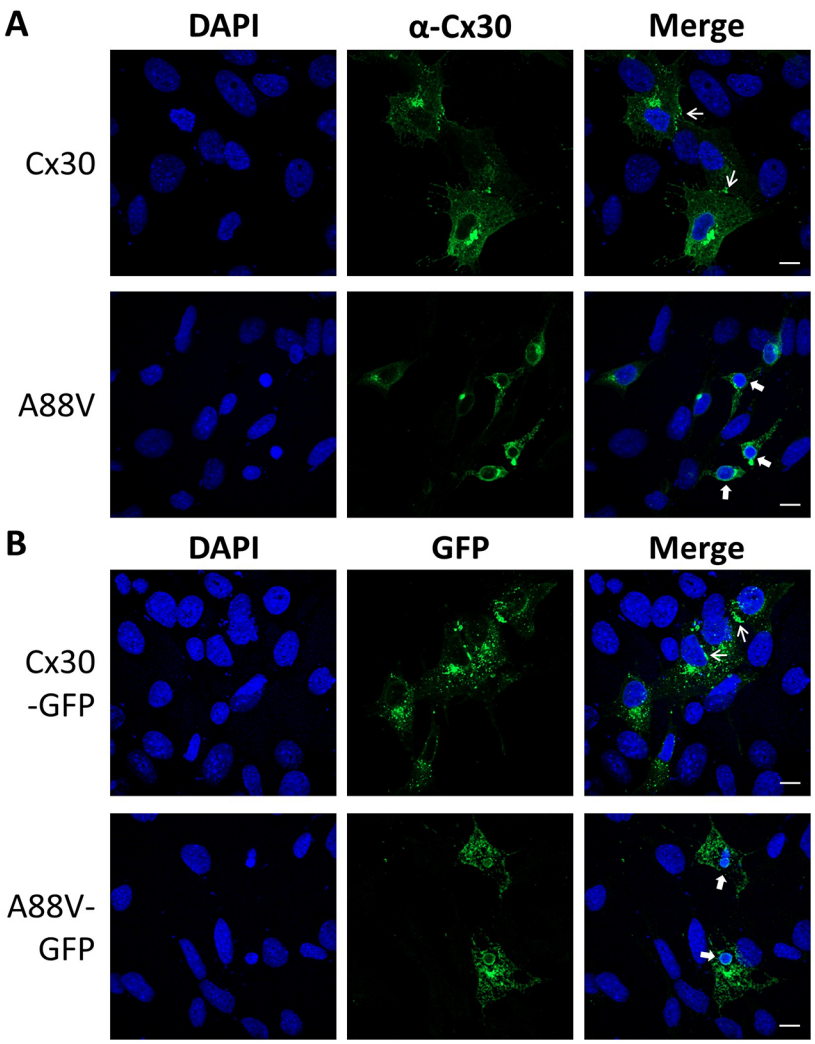

Fig. 1. Cx30-A88V is toxic to HEI-OC-1 cells. (A) HEI-OC1 cells engineered to transiently express untagged or GFP-tagged wild-type Cx30 or the Cx30-A88V mutant (green) were counterstained with Hoechst 33342 (blue) to label nuclei. Cells expressing Cx30 or Cx30–GFP showed normal cell morphology and Cx30 localization to gap junction-like puncta at cell–cell interfaces (thin arrows). Nuclei appeared normal and healthy. (B) In contrast, Cx30-A88V and Cx30-A88V–GFP expressing cells exhibited shrunken cell bodies, a lack of gap junction-like puncta and condensed, pyknotic nuclei (thick arrows), suggesting that the cells expressing the Cx30-A88V mutant were undergoing cell death. Scale bars: 10 µm.

latencies compared to wild-type mice (Fig. 2B) and significantly higher wave I amplitudes across all age sets (Fig. 2C), indicating an overall better neural output from the cochlea. It is important to note that although the homozygous mutant mice showed significantly elevated amplitudes at 6 months of age, they still exhibited an ∼26% age-related decline in neural output at 6 months compared to young mice. However, this pales in comparison to wild-type and heterozygous mice, which had ∼66% and ∼64% age-related reductions in wave I amplitude, respectively. These data indicate that even though there is a slight decline in the hearing profile of homozygous mutant mice with age, they exhibit remarkable, prolonged hearing protection on a mouse background that normally presents with early-onset hearing loss.

Wild-type and mutant mice exhibit normal cochlear development, but reduced Cx30 gap junction plaques in homozygous mice

We next investigated whether there were any differences in the cochlear epithelium and/or hair cell development, as well as Cx30 expression, between the three genotypes at early postnatal ages. Whole cochlear sensory epithelia cultured for 24 h showed normal organ of Corti structure (three rows of outer hair cells and one row of inner hair cells) in both the basal (high frequency) and apical (low frequency) regions of the epithelium (Fig. 3A). At lower magnification, there appeared to be a reduced density of Cx30 gap junction plaques in the homozygous mice in the basal region of the epithelium (Fig. 3A). To investigate this further, same thickness (∼30 µm), high-resolution Airyscan image stacks of Cx30 (green) in basal and apical regions were flattened (Fig. 3B) and magnified (insets, Fig. 3B). Interestingly, the density and size of Cx30 gap junction plaques was reduced in both basal and apical regions of homozygous epithelia, with the difference being more pronounced in the high frequency basal turn regions.

Next, using cochlear cryosections immunostained for Cx30 (green) and counterstained with phalloidin (red) and DAPI (blue) to label actin and nuclei, respectively, we saw no overt differences in the cochlear duct structure in either the basal or apical turns across the genotypes of 3-month-old mice (Fig. 4A). In addition, although the localization of Cx30 did not seem to differ across genotypes, there was an apparent reduction in Cx30 intensity in the type II fibrocyte region of the cochlear lateral wall within the basal turn of homozygous mutant mice (asterisk, Fig. 4A).

To determine whether the reduced endocochlear potential (EP) reported by Lukashkina et al. (2017) in homozygous mice was due to gross malformations in the stria vascularis, we immunostained cryosections for Kir4.1 (green), an intermediate cell-specific potassium channel that is essential for the EP, and counterstained for actin (red) that demarcates the strial unit (Fig. 4B). We found no obvious differences in the structure of the stria vascularis or expression levels of Kir4.1 across genotypes or cochlear turns

Journal of Cell Science (2019) 132, jcs224097. doi:10.1242/jcs.224097

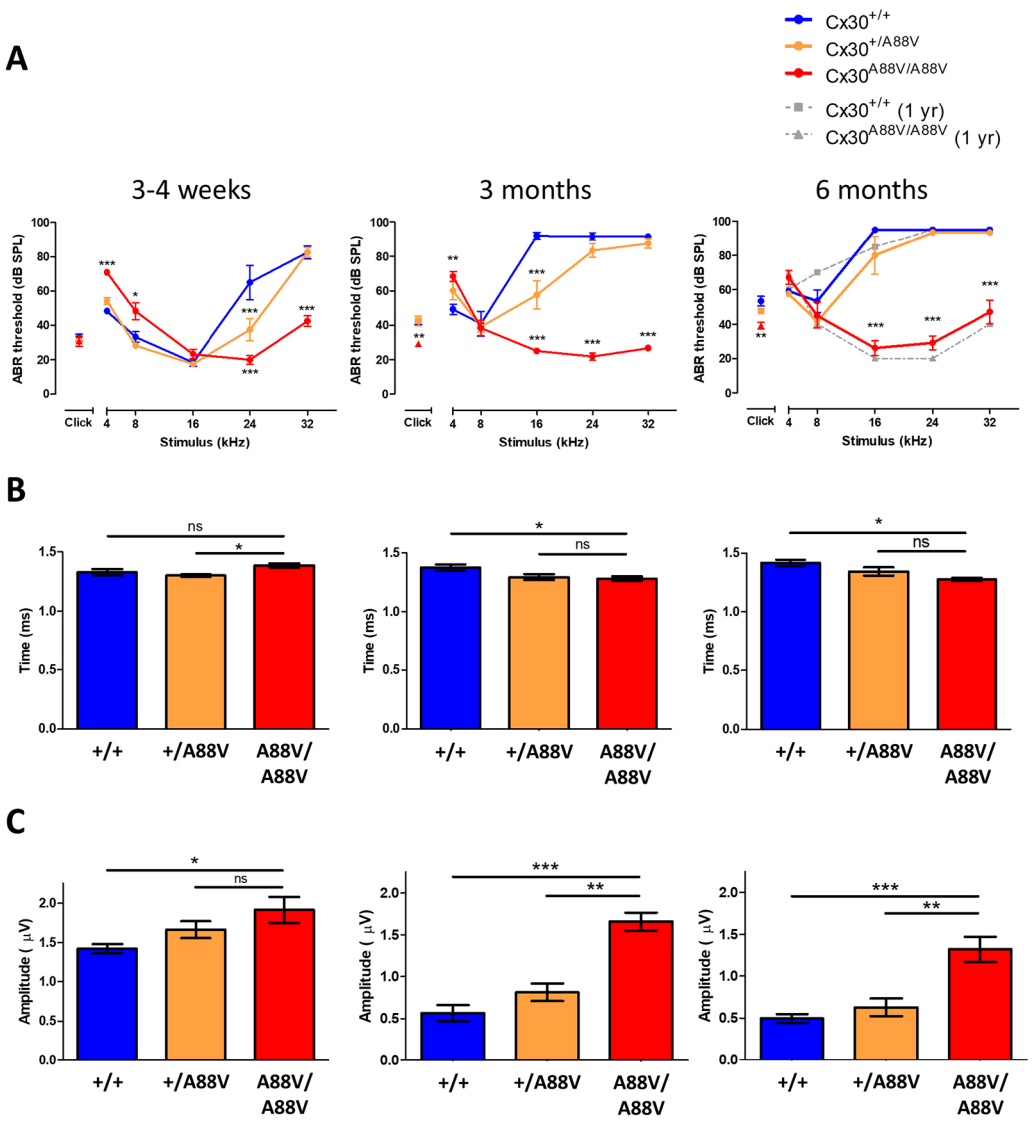

Fig. 2. Aged Cx30$^{A88V/A88V}$ mice are protected against hearing loss. (A) Broadband (click) and frequency-specific ABR profiles of young (3–4 weeks) and aged (3 and 6 months) Cx30$^{+/+}$, Cx30$^{+/A88V}$ and Cx30$^{A88V/A88V}$ CD-1 mice revealed a dramatic early-onset, high frequency hearing loss in Cx30$^{+/+}$ and Cx30$^{+/A88V}$ mice that was protected against in Cx30$^{A88V/A88V}$ mice. ABR data from single 1-year-old Cx30$^{+/+}$ and Cx30$^{A88V/A88V}$ mice (plotted in grey on the 6 month chart) showed hearing protection in the homozygous mutant even at this advanced age. (B) Latencies measured from the onset of the click stimulus to the peak of wave I at 90 dB SPL show improved neural conduction speeds (shorter latencies) in Cx30$^{A88V/A88V}$ mice at 3 and 6 months of age. (C) Wave I click amplitudes at 90 dB SPL also showed consistently higher neural firing/synchrony in Cx30$^{A88V/A88V}$ mice across all age groups, although the average amplitude across all genotypes did decrease with age. *P<0.05, **P<0.01, ***P<0.001 by two-way ANOVA (A) or one-way ANOVA (B,C). N=6 mice per each genotype for each age set. Error bars represent s.e.m.

(Fig. 4B), indicating that the structure of the stria vascularis and expression of Kir4.1 is not disrupted in homozygous mutant mice.

Cx30 mRNA and protein is reduced in Cx30-A88V mutant cochleae

Modifications of the Cx30 gene, *Gjb6*, have been shown to not only influence the mRNA and protein levels of Cx30, but also of Cx26 (Boulay et al., 2013; Ortolano et al., 2008; Schütz et al., 2010). Therefore, we investigated whether the Cx30-A88V gene mutation affected the levels of Cx30 and Cx26 mRNA and protein in whole cochleae extracts. In mice at 4–6 weeks of age, there was a significant decrease in Cx30 mRNA (homozygotes only) and protein levels (heterozygotes and homozygotes) compared to littermate wild-type controls (Fig. 5A,B), but no significant reduction in Cx26 mRNA or protein (Fig. 5A,B). In a similar fashion, in mice at 3 months of age, there were significant reductions in mRNA (homozygotes only) and protein (heterozygotes and homozygotes) for Cx30, but not for Cx26, compared to wild-types (Fig. 6A,B). These data indicate that the Cx30-A88V genetic mutation leads to a downregulation or loss of stability of Cx30 mRNA and/or protein in homozygous mouse cochleae.

A88V mutant mice are protected against hair cell loss

We next determined whether the hearing loss seen in CD-1 wild-type and heterozygote mice is due to hair cell and/or spiral ganglion neural projection loss in adult and aged animals. *Z*-stack orthogonal projections from cochlear cryosections of 3-month-old mice revealed an absence of outer hair cells in the basal turn of wild-type and heterozygote mice, but not in the apical turns (Fig. 7A);

Journal of Cell Science (2019) 132, jcs224097. doi:10.1242/jcs.224097

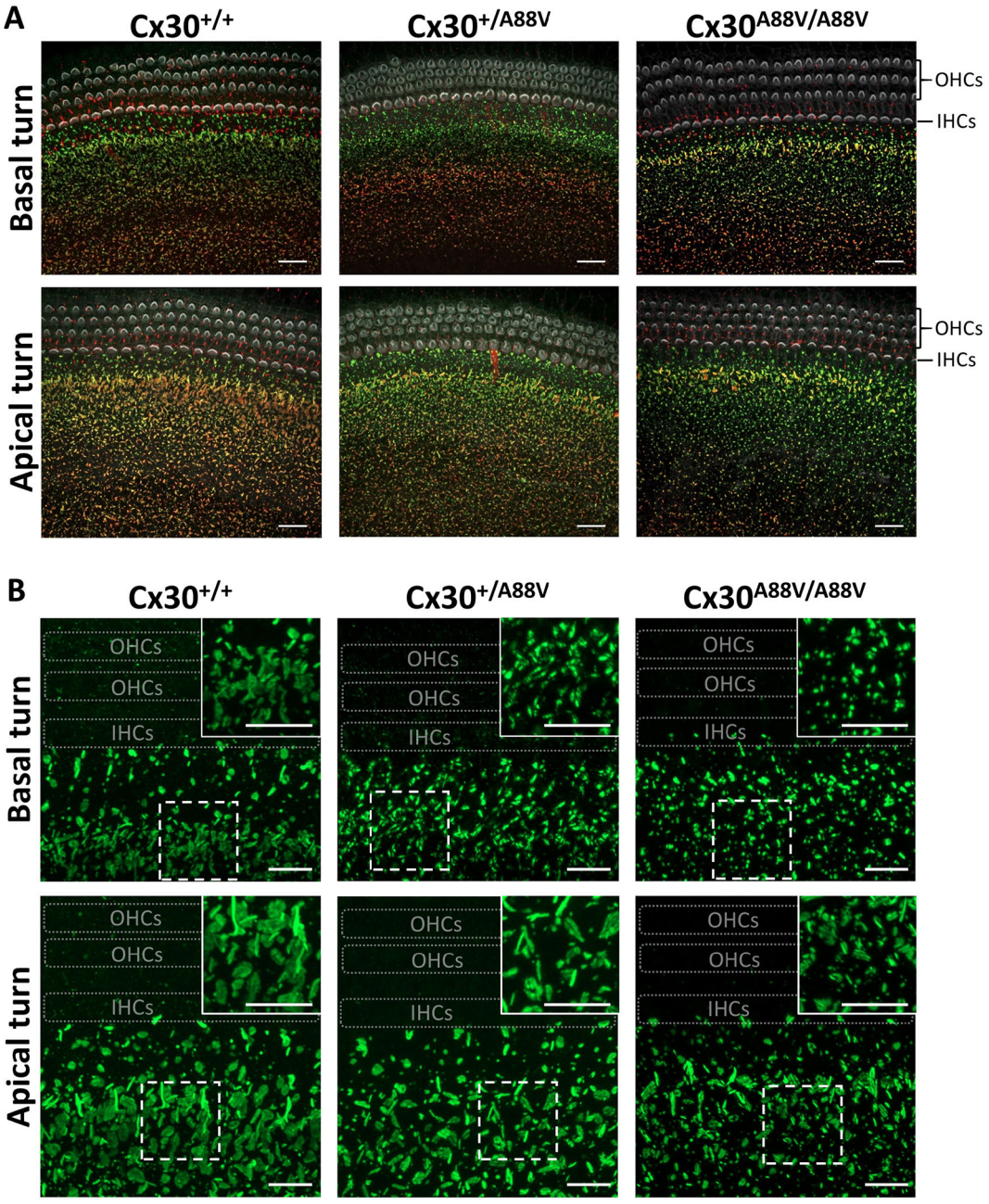

Fig. 3. Organotypic cultures exhibit reduced gap junction expression in neonatal Cx30$^{A88V/A88V}$ mice. (A) Representative full thickness *z*-stack projections of organotypic cultures from 3–4-day-old mouse pups were immunolabelled for Cx26 (red), Cx30 (green) and counterstained with fluorescently tagged phalloidin to demarcate hair cells (white) in basal and apical turns of the cochlear epithelium. There was a normal complement of three rows of outer hair cells (OHCs) and one row of inner hair cells (IHCs) across all genotypes. Scale bars: 20 µm. (B) Same thickness (30 µm), high-resolution Airyscan *z*-stack projections of Cx30 (green) in Kölliker's organ cells showed a consistent decrease in Cx30 plaque density and plaque size in mutant mice. The positions of hair cell rows are marked by the outlined rectangles. Insets represent magnified images within dashed boxes. Scale bars: 10 µm.

findings consistent with the high frequency hearing loss profile observed in these genotypes. In contrast, homozygous Cx30-A88V mice had a normal complement of three rows of outer hair cells and one row of inner hair cells in both basal and apical turns (Fig. 7A). In addition, type II neural projections to the outer hair cells were visible crossing Nuel's space in the basal turn of homozygous mice (arrow, Fig. 7A), which were absent in the basal turns of wild-type and heterozygote mice. Conversely, there were no apparent deficits in the apical turn across all mouse genotypes.

Consistent with the loss of outer hair cells at 3 months of age, whole-mount cochlear epithelia from 6-month-old mice also showed severe loss of outer hair cells and reduced density of inner hair cells in wild-type and heterozygous mice, as determined by actin (phalloidin) and nuclei (DAPI) staining (Fig. 7B). Even at 6 months of age, homozygous mutant mice showed remarkable persistence of inner and outer hair cells in the basal turn, with only a few outer hair cells missing (Fig. 7B). The structure of the epithelium was largely maintained across genotypes in the apical turns. These data indicate that severe hearing loss seen in wild-type and heterozygous Cx30-A88V CD-1 mice was due to a fast progression of hair cell loss in a basal to apical gradient, whereas homozygous mutant mice were protected against hair cell loss.

Journal of Cell Science (2019) 132, jcs224097. doi:10.1242/jcs.224097

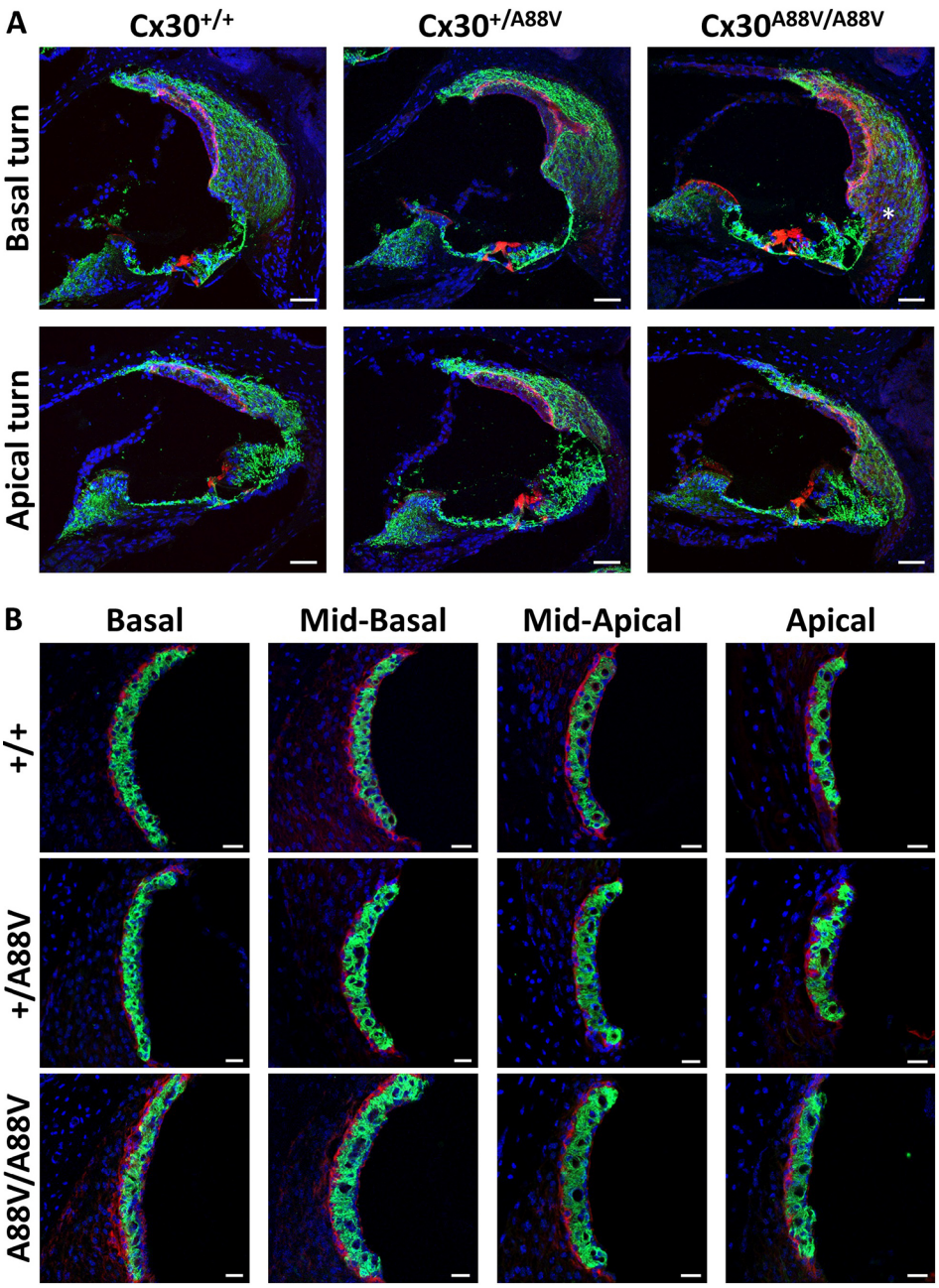

Fig. 4. Cochlear cryosections reveal normal gross anatomy, but reduced Cx30 expression in the lateral wall of 3-month-old mice. (A) Cryosections (18 µm thickness) were immunostained for Cx30 (green) and counterstained with fluorescently tagged phalloidin to label actin (red) and Hoechst 33342 to label nuclei (blue). Representative images of basal and apical turns for all three genotypes are shown. The structure of all the three cochleae from each genotype appeared similar; however, there was a noticeable reduction of Cx30 labelling in fibrocytes resident in the basal turn of the $Cx30^{A88V/A88V}$ lateral wall (asterisk). Scale bars: 50 µm. (B) Cryosections were immunolabelled for Kir4.1 (green), a marker of strial intermediate cells, and counterstained for actin (red, which demarcates strial basal cells) and nuclei (blue). Representative images of the stria vascularis in all turns of the cochlea showed no obvious differences in morphology or Kir4.1 expression. Scale bars: 20 µm.

DISCUSSION

Mutations in the genes that encode Cx26 and Cx30 are most commonly linked to hereditary hearing loss and skin disease, indicating a vital role for these Cxs in normal cochlear and skin physiology (Xu and Nicholson, 2013). Although the Cx30-A88V mutant causes an ectodermal dysplasia known as Clouston syndrome, it has not been reported to cause hearing loss when patients have a normal complement of Cx26 (Jan et al., 2004; Sugiura et al., 2013). This is surprising for two reasons: (1) we and others have shown that the Cx30-A88V mutant is highly toxic to cells when overexpressed in an *in vitro* system (Berger et al., 2014; Essenfelder et al., 2004; Lu et al., 2018), and (2) Cx30 is highly abundant in the inner ear (Ahmad et al., 2003; Forge et al., 2003b; Kikuchi et al., 1995; Lautermann et al., 1998), which suggests that any perturbations in its normal function could have negative consequences in the exquisitely sensitive sensory epithelium (Johnson et al., 2017; Sun et al., 2005; Zhang et al., 2005). In the present study, we aimed to provide an improved understanding of the role Cx30 plays in supporting the cochlear cells that are essential for hearing across a normal lifespan. To that end, we conducted a novel investigation into the effect of the Cx30-A88V mutant on age-related changes in the structure and function of the cochlea using *in vitro* and *in vivo* mouse models.

In our first experimental series, we overexpressed the Cx30-A88V mutant in HEI-OC1 cells to determine whether it would trigger cell death in a hearing-relevant cell line, or alternatively, whether cochlear cells would be resistant to Cx30-A88V-related toxicity. Similar to what we had observed in HeLa and REK cells, the Cx30-A88V mutant drove HEI-OC1 cells into a cell death pathway, possibly due to the overproduction of 'leaky' hemichannels; findings which have been observed previously for this mutant (Essenfelder et al., 2004) as well as for other Cx skin

Journal of Cell Science (2019) 132, jcs224097. doi:10.1242/jcs.224097

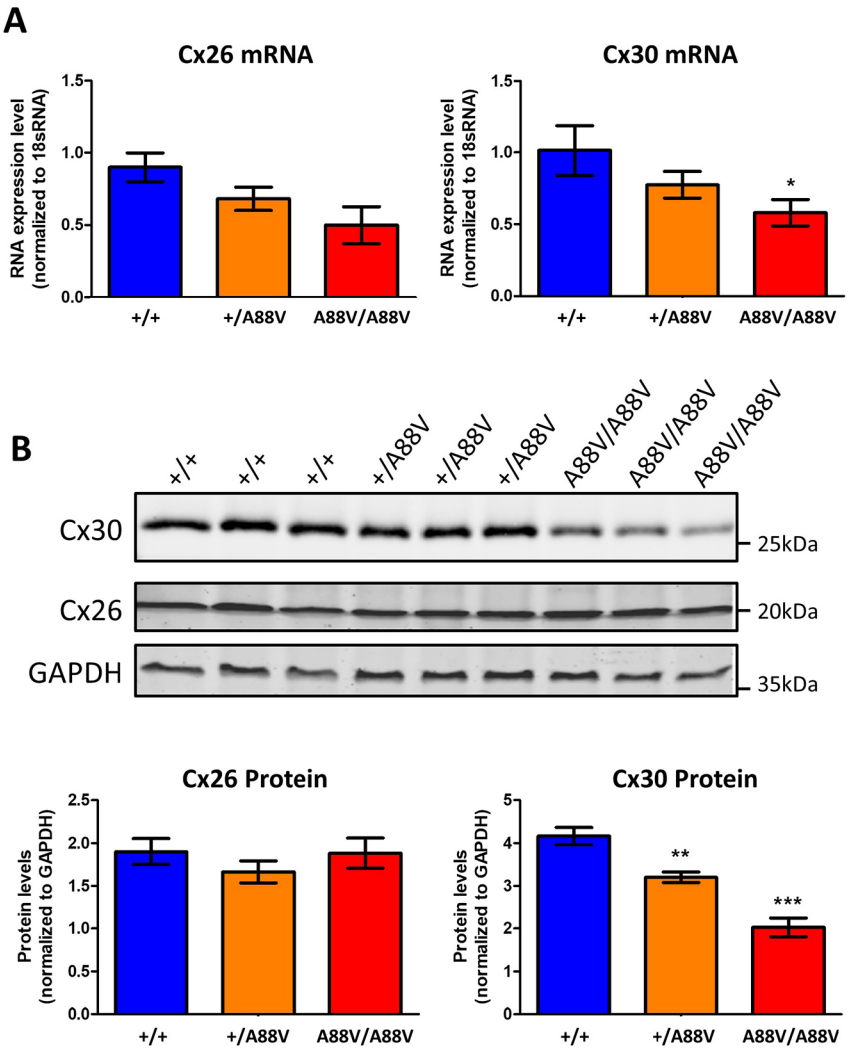

Fig. 5. Four-to-six-week-old Cx30$^{A88V/A88V}$ mice exhibit reduced Cx30 mRNA and protein levels. (A) Cx26 and Cx30 mRNA expression levels were quantified using qPCR and normalized to 18S rRNA. There was a significant reduction of Cx30 mRNA in Cx30$^{A88V/A88V}$ mice compared to Cx30$^{+/+}$. N=3, *P<0.05. (B) Western blot analysis showed a reduction of Cx30 protein levels in Cx30$^{+/A88V}$ and Cx30$^{A88V/A88V}$ cochleae in comparison to wild-type littermate controls (Cx30$^{+/+}$). N=3, **P<0.01, ***P<0.001. Error bars represent s.e.m. A wild-type sample was set as a control.

disease-linked mutants (Chi et al., 2012; García et al., 2015; Mhaske et al., 2013; Retamal et al., 2015). It is worth noting that, despite the toxic effects observed *in vitro*, keratinocytes from homozygous mutant mice appeared healthy, and the skin of these mice exhibited only mild palmoplantar hyperkeratosis (Bosen et al., 2014). These findings strongly argue for studying Cx-linked mutants in mouse models because the dosage of the mutant expressed can dramatically affect the cell phenotype. In this case, the mutant mouse expresses the appropriate levels of the Cx30-A88V mutant given that the endogenous Cx30 promoter remains fully intact, whereas overexpression of the Cx30-A88V mutant presumably drives the toxicity seen in cell lines. Importantly, potential crosstalk between Cx30 mutant expression and its closely related isoform, Cx26, can be investigated in an *in vivo* setting that would mimic the clinical context.

To determine the effect of the Cx30-A88V mutant *in vivo*, we examined Cx30 distribution by immunolabelling the cochleae of neonatal mice, and we also assessed the mRNA and protein levels of Cx30 and Cx26 in whole cochleae extracts from adult mice. Unlike the skin of Cx30-A88V mutant mice, which showed similar Cx30 expression levels to that of wild-type mice (Bosen et al., 2014), in the present study we observed a reduction in the density and size of Cx30 gap junction plaques in cochleae of homozygous mutant mice. It is reasonable to predict that these gap junctions, while present, are likely to be non-functional because the Cx30-A88V mutant has been shown to be incapable of forming functional gap junction channels (Berger et al., 2014). Overall, the altered gap junction morphology in the Cx30-A88V mutant mice corresponded with a reduction in total Cx30 mRNA and protein in the homozygous mutant mice, suggesting that the mutation was destabilizing the Cx30 mRNA, resulting in overall lower Cx30 production.

Previous studies have reported an unusual hearing profile in young adult mice (3–9 weeks old) expressing the homozygous Cx30-A88V mutant (Bosen et al., 2014; Lukashkina et al., 2017), whereby they were protected from the early-onset, high frequency hearing loss inherent to wild-type mice on the CD-1 background. Furthermore, homozygous Cx30-A88V mutant mice had a greatly reduced level of cochlear amplification linked to their outer hair cells (Bosen et al., 2014; Lukashkina et al., 2017); findings which at first may seem inconsistent with the preserved hearing thresholds in these mutants, yet ultimately suggestive of a role for Cx30 gap junctions in sensory processing. However, it remained unclear whether other mechanisms contributed to the preservation of high frequency hearing in young mutant mice, such as compensatory Cx expression, or whether aging mutant mice would eventually revert to similar hearing loss levels as those found in wild-type or heterozygous mice. In addressing these issues in the present study, we confirmed the previously-reported hearing preservation in young homozygous mutant mice (Bosen et al., 2014; Lukashkina

Journal of Cell Science (2019) 132, jcs224097. doi:10.1242/jcs.224097

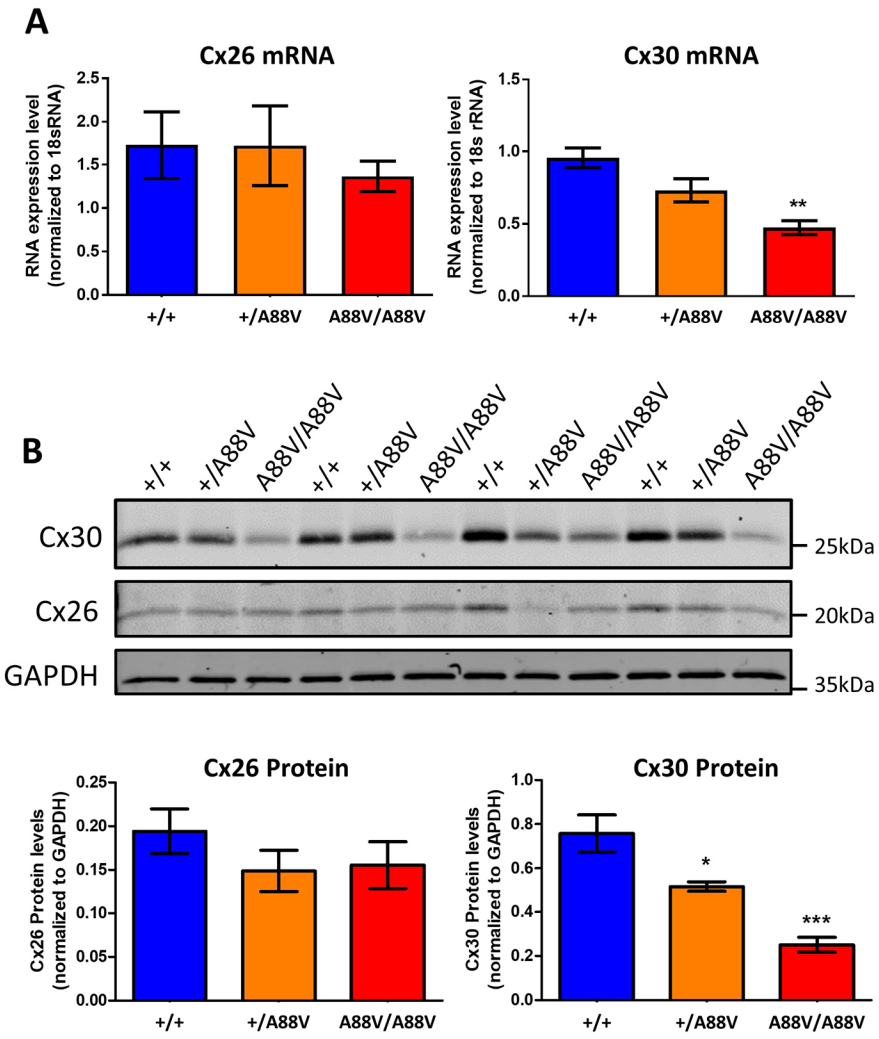

Fig. 6. Three-month-old Cx30$^{A88V/A88V}$ mice have reduced Cx30 mRNA and protein levels. (A) Cx26 and Cx30 mRNA expression levels of were quantified using qPCR and normalized to 18S rRNA. There was a significant reduction of Cx30 mRNA in Cx30$^{A88V/A88V}$ mice compared to Cx30$^{+/+}$. N=4, $^{**}P$<0.01. (B) Western blot analysis showed a consistent reduction of Cx30 protein levels in Cx30$^{+/A88V}$ and Cx30$^{A88V/A88V}$ cochleae in comparison to wild-type littermate controls (Cx30$^{+/+}$). N=4, $^{*}P$<0.05, $^{***}P$<0.001. Error bars represent s.e.m.

et al., 2017), and we have shown for the first time that the Cx30-A88V mutant confers long-term protection to high frequency hearing in aged mice (6 months old), with evidence of hearing protection even at 1 year old. Furthermore, given that the homozygous Cx30-A88V mutant mice in the present study maintained nearly a full complement of outer hair cells in older age as well as preserved ABR wave I amplitudes and latencies, and young mutants showed greater cochlear sensitivity (as revealed by their distortion product otoacoustic emissions) (Bosen et al., 2014; Lukashkina et al., 2017) than their wild-type littermates, it is reasonable to predict that higher-level auditory processing may also be preserved in the aged mutants. For example, unlike wild-type mice on the CD-1 background, Cx30-A88V mutant mice could be expected to show a well-preserved sensitivity to the spectrotemporal features of sound in their environment, including accurate frequency discrimination and temporal processing (e.g. gap detection); features known to be impaired following outer hair cell loss and/or damage (Oxenham and Bacon, 2003). That said, future studies would be needed to determine whether such higher-level auditory processing is indeed spared in the homozygous mutant mice because Cx30 is also expressed in astrocytes throughout the central auditory pathway (Nagy et al., 1999).

At present, the reason(s) for the preservation of hearing in the aged homozygous Cx30-A88V mutant mice is unclear. On first thought, one might argue that a loss or dramatic reduction of Cx30-A88V function would prevent the passage of small cellular signals that might ultimately contribute to the hair cell death we observed in the wild-type mice. However, this explanation is not likely to be sufficient, given that the hair cells are isolated from the gap junctional networks found in the organ of Corti, and should not directly receive any cell death signals that might pass through a gap junction. A second explanation may involve hyperactive Cx30-A88V hemichannels, as shown previously in HeLa cells (Essenfelder et al., 2004), that release ATP or other small molecules from the supporting cells of the organ of Corti to the extracellular milieu. That said, this process would be expected to lead to supporting cell death, and ultimately to a general deterioration in integrity of the organ of Corti; findings that were not observed even in aged mutant mice. In fact, both the inner and outer hair cells in the organ of Corti of the homozygous Cx30-A88V mutants were found to be healthy, in contrast to the extensive cell loss seen in wild-type mice. A third possibility rests on the prospect of a Cx feedback system where the loss of Cx30 function and protein level would dramatically drive the increased expression and stability of the closely related Cx26, as this level of regulation in the cochlea has been previously reported (Boulay et al., 2013; Ortolano et al., 2008). However, in both young and aged heterozygous or homozygous mutant mice this was not the case as Cx26 mRNA and protein levels remained unchanged, although the functional activity of Cx26 was not directly examined. Finally, because the Cx30-A88V mutant has

Journal of Cell Science (2019) 132, jcs224097. doi:10.1242/jcs.224097

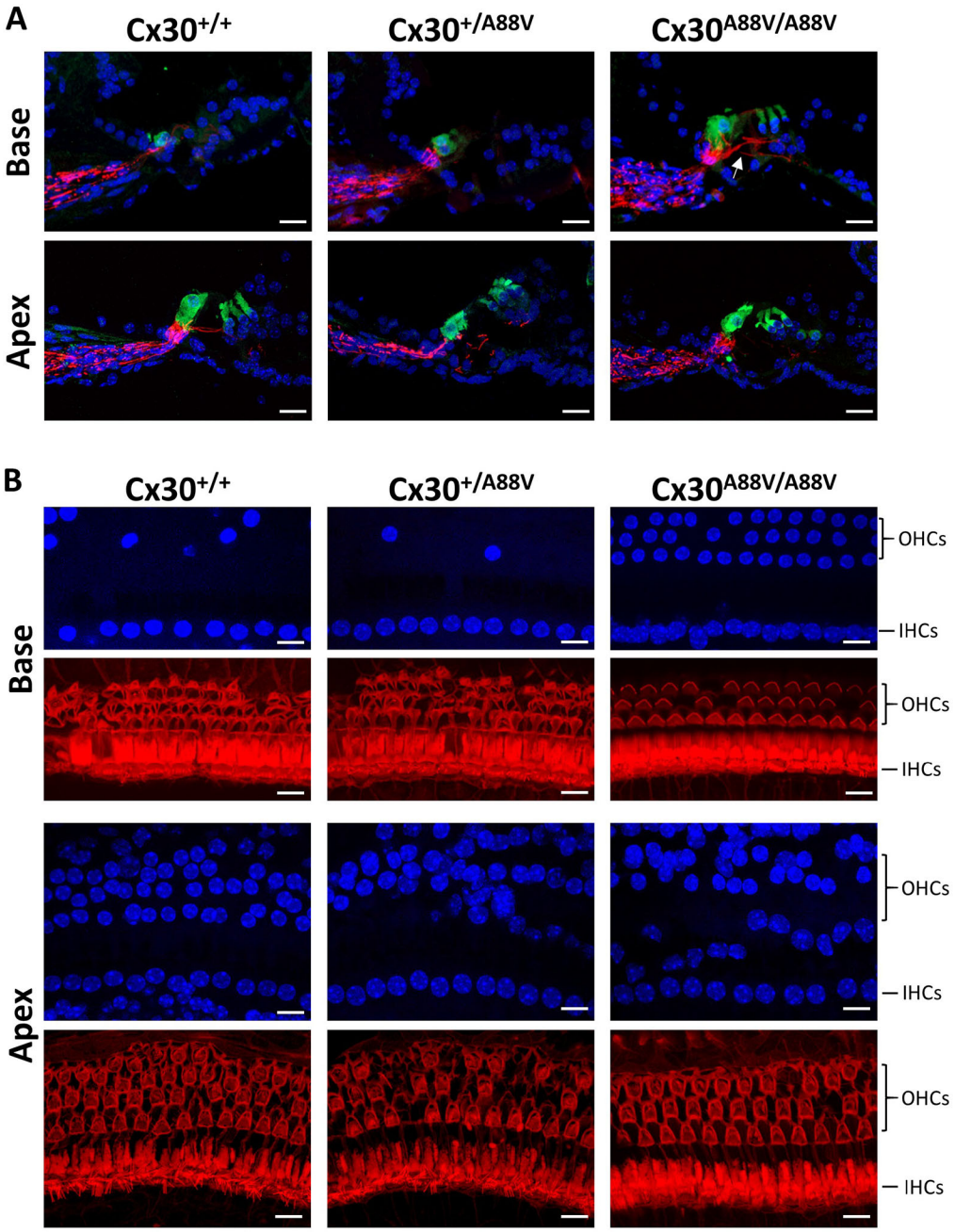

Fig. 7. Aged Cx30$^{A88V/A88V}$ mice are protected against neuronal and hair cell loss. (A) Cochlear cryosections from 3-month-old mice were immunolabelled for myosin-VI to highlight hair cells (green) and neurofilament to label neurons (red), and counterstained with Hoechst 33342 to label nuclei (blue). The basal turns of Cx30$^{+/+}$ and Cx30$^{+/A88V}$ mice lacked outer hair cells, whereas Cx30$^{A88V/A88V}$ mice had preserved hair cells and neural projections crossing Nuel's space to outer hair cells (arrow). Apical turns appeared similar between genotypes. Scale bars: 20 µm. (B) *Z*-stack projections from cochlear whole-mounts from 6-month-old mice. Hair cells were labelled with fluorescently tagged phalloidin (red) and counterstained with Hoechst 33342 to label nuclei (blue). There was extensive loss of outer hair cells in the basal turns of Cx30$^{+/+}$ and Cx30$^{+/A88V}$ mice, as evidenced by the lack of V-shaped stereocilia bundles on the apical surface and nuclei in the baso-lateral region of hair cells. In contrast, almost all basal turn outer hair cells in Cx30$^{A88V/A88V}$ mice had normal stereocilia bundles and nuclei. Scale bars: 10 µm.

been linked to cytotoxicity, one might speculate that the reduced levels of Cx30 mRNA and protein may represent a negative feedback loop whereby the cells protect themselves against cell death by downregulating toxic signals from entering or disseminating amongst supporting cells. In support of this notion, reducing functional Cx30 levels in the cochlea can be well tolerated as we know that *Gjb6* gene-ablated mice hear normally (Boulay et al., 2013).

The discovery that homozygous Cx30-A88V mice exhibit better high frequency hearing than wild-type mice on the shared CD-1 background is all the more remarkable since the mutant mice also exhibit a reduced EP (Lukashkina et al., 2017) – the positive potential in the endolymphatic space (+80 to 100 mV) that is created by the stria vascularis, and is thought to be essential for hair cell transduction and hearing sensitivity (Nin et al., 2008). In considering the Cx30-A88V-related reduction in the EP, Lukashkina and colleagues proposed a novel mechanism that may contribute to the preserved hearing sensitivity observed in these Cx30-A88V mutant mice (Lukashkina et al., 2017). It was suggested that the electromotility of the outer hair cells – a crucial feature for hearing sensitivity – could be driven by extracellular potentials in their vicinity, instead of solely by current flux through their mechanotransducer channels. It was presumed that this alternative method of facilitating outer hair cell electromotility was possible thanks to an accumulation of cations and, consequently, extracellular potentials, that resulted from a Cx30-A88V mutation-related impairment in the electrical coupling through gap junctions in the sensory epithelium. Ultimately, the reduced expression of Cx30 that we observed in the Cx30-A88V mutant mice in the present study provides some support for the aforementioned hypothesis by Lukashkina and colleagues (2017).

To address the unresolved issue of how the Cx30-A88V mutant may indeed be causing a reduction in the EP in mutant mice, we immunolabelled cochlear cryosections and assessed the gross morphology of the cochlear lateral wall, as well as the expression of Kir4.1, an inwardly rectifying potassium channel found in the apical membrane of intermediate cells in the stria vascularis that is believed to be essential for EP development and maintenance (Chen and Zhao, 2014; Marcus et al., 2002). Surprisingly, we found no obvious differences in the morphology of the cochlear lateral wall, including the stria vascularis, between the three genotypes. Moreover, contrary to our prediction, there did not appear to be a reduced expression of Kir4.1 in the mutant mice that could account for the reduced EP reported previously (Lukashkina et al., 2017). Because several Cx26 and/or Cx30 mutant mouse models also exhibit reduced or absent EPs (Cohen-Salmon et al., 2002; Schutz et al., 2011; Teubner et al., 2003), it will be of considerable interest for future studies to further investigate the underlying cellular mechanism(s) by which these Cxs influence the EP.

Intriguingly, there are no reports of Clouston syndrome patients suffering from hearing loss, suggesting that a single allele encoding the Cx30-A88V mutant in this autosomal dominant disease can manifest as skin disease with no effect on hearing. Patients have not been identified that have two alleles that encode the Cx30-A88V mutant, but if they existed, the mouse studies suggest that they would be protected from age-related hearing loss. That said, it is highly debatable whether one copy would be sufficient to prevent hearing loss in old age.

In conclusion, this study has shown for the first time that the 40–60 dB SPL high frequency hearing protection seen in young adult Cx30-A88V mice is remarkably persistent in aged animals, and therefore does not just represent a delay in hearing loss. We suggest that the protection is conferred by the mutation causing an overall reduction in Cx30, but not Cx26, RNA and protein levels within the cochlea. Importantly, this leads to protection against hair cell and neuronal death in mutant mice. The mechanism of this protection, however, remains to be determined. It would also be intriguing to see whether Clouston syndrome patients expressing the Cx30-A88V mutant exhibit better than normal hearing thresholds during aging. Ultimately, our collective results suggest that targeting the downregulation of Cx30 in the cochlea might be a therapeutic option for the prevention of age-related hearing loss.

MATERIALS AND METHODS

Cell culture and constructs

HEI-OC1 cells (kindly provided by Dr Federico Kalinec, Department of Head and Neck Surgery, David Geffen School of Medicine, UCLA, USA) were cultured under permissive conditions (33°C and 10% CO_2) in Dulbecco's Modified Eagle's medium (DMEM; Sigma-Aldrich), containing 10% fetal bovine serum (FBS; Thermo Fisher) without antibiotics. Mouse Cx30 wild-type and Cx30-A88V cDNA constructs with and without eGFP were made as previously described (Berger et al., 2014). The Cx30 constructs were transfected into HEI-OC1 cells using *Trans*IT-LT1 (Mirus) transfection reagent (1.5 µg DNA: 3 µl reagent in 6-well plates) for ∼18 h. Cells were fixed in 4% paraformaldehyde (PFA) for 15 min at room temperature then blocked and permeabilized in 3% bovine serum albumin (BSA) and 0.1% Triton X-100. Cells expressing Cx30 without eGFP were then incubated overnight at 4°C in rabbit anti-Cx30 antibody (1:400; Thermo Fisher, 71-2200) and mouse anti-GM130 (1:500; BD Transduction Laboratories, 610822). Coverslips were then washed and incubated with anti-rabbit Alexa Fluor 488 (1:500; Thermo Fisher, A11008) and anti-mouse Alexa Fluor 555 (1:500, Thermo Fisher, A32727) secondary antibodies for 1 h. All coverslips were counterstained with the nuclear marker Hoechst 33342 and mounted in ProLong Gold Antifade Mountant (Thermo Fisher, P36934). Confocal images were acquired using a LSM800 Zeiss confocal microscope.

Mice

$Cx30^{+/A88V}$ and $Cx30^{A88V/A88V}$ mice were generated as previously described (Bosen et al., 2014) and generously provided by Dr Klaus Willecke (Life and Medical Sciences Institute, Bonn, Germany). Mice were crossed several times with CD-1 mice to generate a CD-1 background of ∼88%. Genotypes of wild-type, $Cx30^{+/A88V}$ and $Cx30^{A88V/A88V}$ mice were confirmed by means of gel electrophoresis of PCR products using the following primers: forward, 5′-GGTCGAAGGAACCTTTCACAGG-3′ and reverse, 5′-GCTACCATC-ACGTGCTCTTTGG-3′, which give rise to bands of 423 bp (wild-type) and 481 bp (A88V). Male mice used in this study were housed in the animal care facilities at the University of Western Ontario and maintained on a 12 h/12 h dark/light cycle with food and water provided *ad libitum*. All experiments were approved by the Animal Care Committee at the University of Western Ontario.

Hearing assessment with the auditory brainstem response (ABR)

Hearing levels were assessed using the ABR technique, which measures the electrical activity in the brainstem evoked by the repeated presentation of a given acoustic stimulus. Five different acoustic stimuli were used for this study, including a broadband click stimulus, and 8, 16, 24 and 32 kHz tonal stimuli to assess both broadband (click) and tonal-specific hearing frequencies. Three different age groups of mice were used: 3–4 weeks, 3 months and 6 months. In one case, 1-year-old mice were assessed. A detailed description of the experimental procedures for ABR recordings was previously described (Abitbol et al., 2016). Briefly, mice were deeply anaesthetized with 100 mg/kg ketamine and 10 mg/kg xylazine via intraperitoneal injections. Supplemental half doses were administered as necessary throughout the recordings. Electrical recordings of ABRs were acquired through subdermal electrodes placed at the vertex (active electrode), the mastoid of the right ear (reference electrode) and on the mid-back (ground electrode). The body temperature of mice was maintained at ∼37°C on a digital homeothermic heating pad throughout the experiment. ABR thresholds were determined as the quietest sound stimulus that elicited a peak in the ABR waveform. For further analysis, BioSig software (Tucker-Davis Technologies) was used to measure the amplitudes (which is the number and synchrony of neurons firing) and latencies (which measures the conductive speed of neurons) of the peak of the first wave of the ABR. These auditory nerve measurements were elicited by the 90 dB SPL click stimulus for all genotypes tested. All ABR waveform measurements were conducted on raw ABR traces.

Organotypic cochlear cultures

Organotypic cochlear explant cultures were prepared from the cochleae of postnatal day 1–3 mouse pups from a modified protocol previously described (Mann et al., 2009). Briefly, pups were euthanized by decapitation and the pup heads surface-sterilized in 80% ethanol for 10 min. The heads were removed from the ethanol and placed in ice-cold Leibovitz's L-15 medium (Thermo Fisher) where they were midsagitally bisected, brain removed and cochlear bulla gently extracted. The cochlear capsule and lateral wall were removed, leaving the organ of Corti and the greater epithelial ridge attached to the modiolus. The organ of Corti was gently peeled away from the modiolus and plated onto 14 mm diameter glass MatTek dishes (MatTek Corporation) pre-coated with Cell-Tak (Corning) diluted in 0.1 mM $NaHCO_3$ to a final concentration of 70 µg/ml for adhesion. Explants were immersed in DMEM/F12 medium (Thermo Fisher) supplemented with 5% FBS. Cultures were incubated at 37°C and 5% CO_2 for 24 h and then fixed with 4% PFA for 20 min at room temperature. Cultures were then blocked and permeabilized using 3% BSA+0.2% Triton X-100 and incubated with mouse anti-Cx26 (1:300; Thermo Fisher, 33-5800) and/or rabbit anti-Cx30 (1:400; Thermo Fisher, 71-2200) overnight at 4°C. Goat anti-mouse Alexa Fluor 488 and goat anti-rabbit Alexa Fluor 633 (1:500; Thermo Fisher, A11001, A21070) were used to visualize gap junctions, whilst an Alexa Fluor 555 phalloidin stain (1:400; Thermo Fisher, A34055) was used to visualize hair cell stereocilia. Confocal *z*-stacks and high-resolution Airyscan images were taken on an LSM800 confocal microscope (Zeiss) fitted with highly sensitive GaAsP detectors. Images were taken at 1.0–1.3 µm increments with a 63×/1.40 NA oil immersion lens either at 0.5× (confocal) or 1.3× (Airyscan) zoom. The full

thickness of the tissue (from 35 to 61 µm for Fig. 3A) was imaged at 1.0–1.3 µm increments and flattened into a 2D image using ZEN Blue software (Zeiss). Tissue thickness was kept to ∼30 µm for images in Fig. 3B.

Cryosectioning and immunofluorescent labelling of cochleae

Following ABR recordings, mice were euthanized and cochleae were dissected. A small incision was made in the cochlear bone near the apical turn and 4% PFA was gently perfused through both the round and oval windows of the cochleae, which were then bathed in 4% PFA overnight at 4°C and subsequently washed with PBS. Cochleae were decalcified in 4% EDTA for ∼3 days and upon full decalcification were immersed in 30% sucrose overnight for cryopreservation. Each cochlea was embedded in an agarose solution, flash-frozen, and allowed to acclimate in a cryostat (Leica) at −25°C. Sections were cut at 18 µm thickness and stored at −20°C until use. Slides were blocked and permeabilized in 3% BSA+0.2% Triton X-100 solution. Subsequently, slides were incubated with primary antibodies overnight at 4°C. These primary antibodies included rabbit anti-Cx30 (1:400; Thermo Fisher, 71-2200), rabbit anti-Kir4.1 (1:400; Alomone Labs, APC-035), mouse anti-neurofilament (1:200; Sigma-Aldrich, N5389). Slides were then washed and incubated with an appropriate fluorescently conjugated Alexa Fluor secondary antibody (1:500; Thermo Fisher). Subsequently, slides were stained with Hoechst to visualize nuclei.

Quantitative reverse-transcription polymerase chain reaction

Following euthanasia of mice by CO_2, cochleae were dissected and flash-frozen in liquid nitrogen. RNA was extracted from tissues using a combination of Trizol (Thermo Fisher) and an RNeasy kit (Qiagen) as was previously described (Abitbol et al., 2016). A Nanodrop spectrophotometer was used to measure the absorbance of RNA, which was then converted to cDNA using a SuperScript VILO cDNA synthesis kit (Thermo Fisher). Quantitative polymerase chain reactions (qPCRs) were performed using a SYBR Green PCR master mix (Thermo Fisher) in order to quantify mRNA transcript expression of Cx26 and Cx30. The following primers were used: Cx26-specific primers (forward, 5′-CCGTCTTCATGTACGTCTTTTAC-AT-3′ and reverse, 5′-ATACCTAACGAACAAATAGCACAGC-3′) and Cx30-specific primers (forward, 5′-GGCCGAGTTGTGTTACCTGCT-3′ and reverse, 5′-TCTCTTTCAGGGCATGGTTGG-3′). 18S ribosomal ribonucleic acid (rRNA) was used as a housekeeping gene (forward, 5′-GTAACCCGTTGAACCCCATT-3′ and reverse, 5′-CCATCCAATCGGT-AGTAGCG-3′). The PCR thermal profile for all primers was as follows: 50°C for 2 min, 95°C for 2 min, 95°C for 5 s, 60°C for 15 s, followed by a melt curve. Expression of transcripts were normalized to 18S rRNA for quantification.

Protein extraction and immunoblotting

Following euthanasia of mice by CO_2, cochleae were dissected, flash-frozen in liquid nitrogen and either stored at −80°C or processed immediately. Frozen cochleae were crushed with a mortar and pestle on dry ice with liquid nitrogen, as we previously described (Abitbol et al., 2016). TRIzol (Thermo Fisher) extraction was performed to separate RNA, DNA and protein components of the tissue, as per manufacturer's instructions. Protein was isolated by using a series of wash steps including addition of phenol-ethanol, wash solution consisting of 0.3 M guanidine hydrochloride in 95% ethanol, and the protein pellet collected by centrifugation. The pellet was then resuspended in 1% SDS+protease and phosphatase inhibitors, and protein yield determined using the bicinchoninic acid (BCA) assay kit. Equal amounts of protein (20 µg) were run on 10% polyacrylamide gels using SDS-PAGE and transferred to nitrocellulose membranes using an iBlot transfer apparatus (Thermo Fisher). Membranes were blocked with 3% BSA in PBS-Tween (1× PBS, 0.05% Tween 20) for 1 h. Blots were then probed at room-temperature for 2 h or overnight at 4°C with rabbit anti-Cx30 (1:3000; Thermo Fisher, 71-2200), mouse anti-Cx26 (1:1000; Thermo Fisher, 33-5800) and mouse anti-GAPDH (1:10,000; Chemicon, MAB374) antibodies. Blots were washed and incubated for one hour with goat anti-mouse Alexa Fluor 680 secondary antibody (1:10,000; Thermo Fisher) for Cx26 and GAPDH, anti-rabbit IRdye 800CW (1:10,000; LI-COR Biosciences, 926-32211) was used for Cx30. Membranes were visualized with an Odyssey infrared imaging system (LI-COR). Quantitative analysis was performed using Odyssey software (LI-COR) to assess the amount of Cx30 and Cx26 protein. GAPDH was used as a loading control and a reference protein for quantitative analysis.

Whole-mount dissection and immunofluorescence of adult mouse cochlea

Following euthanasia of mice by CO_2, temporal bones were dissected and the cochleae were isolated. A small needle was used to perforate a hole in the apex of the cochlear bone and 4% PFA was gently perfused through the round and oval windows. Cochleae were submersed in 4% PFA overnight at 4°C. After fixation, cochleae were rinsed in PBS and decalcified in 4% EDTA for 3–4 days or until cochleae were fully decalcified. Whole-mount dissections of adult cochlear turns were prepared as follows. Firstly, a piece of a razor blade was used to bisect the cochlea. Tissue connections, Reissner's membrane and tectorial membrane were then peeled away with #55 fine forceps (Fisher Scientific). Razor blade pieces in a blade holder were used to dissect away lateral wall and excess spiral ganglion tissue to leave approximately six segments of the cochlear epithelium from base to apex. Whole-mount sections were blocked and permeabilized with 3% BSA+0.2% Triton X-100 for one hour. Various primary antibodies were incubated overnight at 4°C including rabbit anti-myosin-VI (1:200; Proteus Biosciences, 25-6791), and rabbit anti-Cx30 (1:400; Thermo Fisher, 71-2200). Alexa Fluor secondary antibodies (Thermo Fisher) were used as well as a phalloidin-conjugated stain to visualize hair cell stereocilia as described above in organotypic cochlear cultures. Finally, Hoechst 33342 was used to label nuclei and whole-mount cochleae were mounted and imaged on an LSM800 confocal microscope.

Acknowledgements

The authors would like to thank Dr Klaus Willecke for providing the $Cx30^{+/A88V}$ mutant mice used in this study. The authors also thank Dr Federico Kalinec for generously supplying the HEI-OC1 cells.

Competing interests

The authors declare no competing or financial interests.

Author contributions

Conceptualization: J.J.K., D.W.L., B.L.A.; Methodology: J.J.K., J.M.A., S.H., E.R.P.; Formal analysis: J.J.K., J.M.A.; Writing - original draft: J.J.K., J.M.A., D.W.L., B.L.A.; Writing - review & editing: J.J.K., J.M.A., D.W.L., B.L.A.; Supervision: D.W.L., B.L.A.; Funding acquisition: D.W.L., B.L.A.

Funding

D.W.L. and B.L.A. were funded by Canadian Institutes of Health Research (grant 148584). J.M.A. was funded by a Natural Sciences and Engineering Research Council of Canada Studentship.

Supplementary information

Supplementary information available online at
http://jcs.biologists.org/lookup/doi/10.1242/jcs.224097.supplemental

References

Abitbol, J. M., Kelly, J. J., Barr, K., Schormans, A. L., Laird, D. W. and Allman, B. L. (2016). Differential effects of pannexins on noise-induced hearing loss. *Biochem. J.* **473**, 4665-4680.

Ahmad, S., Chen, S., Sun, J. and Lin, X. (2003). Connexins 26 and 30 are co-assembled to form gap junctions in the cochlea of mice. *Biochem. Biophys. Res. Commun.* **307**, 362-368.

Alexander, D. and Goldberg, G. (2003). Transfer of biologically important molecules between cells through gap junction channels. *Curr. Med. Chem.* **10**, 2045-2058.

Anselmi, F., Hernandez, V. H., Crispino, G., Seydel, A., Ortolano, S., Roper, S. D., Kessaris, N., Richardson, W., Rickheit, G., Filippov, M. A. et al. (2008). ATP release through connexin hemichannels and gap junction transfer of second messengers propagate Ca2+ signals across the inner ear. *Proc. Natl. Acad. Sci. USA* **105**, 18770-18775.

Baris, H. N., Zlotogorski, A., Peretz-Amit, G., Doviner, V., Shohat, M., Reznik-Wolf, H. and Pras, E. (2008). A novel GJB6 missense mutation in hidrotic ectodermal dysplasia 2 (Clouston syndrome) broadens its genotypic basis. *Br. J. Dermatol.* **159**, 1373-1376.

Berger, A. C., Kelly, J. J., Lajoie, P., Shao, Q., Laird, D. W., Paul, D. L., Munro, C. S., Uitto, J., Hodgins, M. B. and Richard, G. (2014). Mutations in Cx30 that

are linked to skin disease and non-syndromic hearing loss exhibit several distinct cellular pathologies. *J. Cell Sci.* **127**, 1751-1764.
Bosen, F., Schütz, M., Beinhauer, A., Strenzke, N., Franz, T. and Willecke, K. (2014). The Clouston syndrome mutation connexin30 A88V leads to hyperproliferation of sebaceous glands and hearing impairments in mice. *FEBS Lett.* **588**, 1795-1801.
Boulay, A.-C., del Castillo, F. J., Giraudet, F., Hamard, G., Giaume, C., Petit, C., Avan, P. and Cohen-Salmon, M. (2013). Hearing is normal without Connexin30. *J. Neurosci.* **33**, 430-434.
Chan, D. K. and Chang, K. W. (2014). GJB2-associated hearing loss: systematic review of worldwide prevalence, genotype, and auditory phenotype. *Laryngoscope* **124**, E34-E53.
Chen, J. and Zhao, H.-B. (2014). The role of an inwardly rectifying K(+) channel (Kir4.1) in the inner ear and hearing loss. *Neuroscience* **265**, 137-146.
Chen, N., Xu, C., Han, B., Wang, Z.-Y., Song, Y.-L., Li, S., Zhang, R.-L., Pan, C.-M. and Zhang, L. (2010). G11R mutation in GJB6 gene causes hidrotic ectodermal dysplasia involving only hair and nails in a Chinese family. *J. Dermatol.* **37**, 559-561.
Chi, J., Li, L., Liu, M., Tan, J., Tang, C., Pan, Q., Wang, D. and Zhang, Z. (2012). Pathogenic connexin-31 forms constitutively active hemichannels to promote necrotic cell death. *PLoS ONE* **7**, e32531.
Cohen-Salmon, M., Ott, T., Michel, V., Hardelin, J.-P., Perfettini, I., Eybalin, M., Wu, T., Marcus, D. C., Wangemann, P., Willecke, K. et al. (2002). Targeted ablation of connexin26 in the inner ear epithelial gap junction network causes hearing impairment and cell death. *Curr. Biol.* **12**, 1106-1111.
Essenfelder, G. M., Bruzzone, R., Lamartine, J., Charollais, A., Blanchet-Bardon, C., Barbe, M. T., Meda, P. and Waksman, G. (2004). Connexin30 mutations responsible for hidrotic ectodermal dysplasia cause abnormal hemichannel activity. *Hum. Mol. Genet.* **13**, 1703-1714.
Forge, A., Marziano, N. K., Casalotti, S. O., Becker, D. L. and Jagger, D. (2003a). The inner ear contains heteromeric channels composed of cx26 and cx30 and deafness-related mutations in cx26 have a dominant negative effect on cx30. *Cell Commun. Adhes.* **10**, 341-346.
Forge, A., Becker, D., Casalotti, S., Edwards, J., Marziano, N. and Nevill, G. (2003b). Gap junctions in the inner ear: comparison of distribution patterns in different vertebrates and assessement of connexin composition in mammals. *J. Comp. Neurol.* **467**, 207-231.
Fraser, F. C. and Der Kaloustian, V. M. (2001). A man, a syndrome, a gene: Clouston's hidrotic ectodermal dysplasia (HED). *Am. J. Med. Genet.* **100**, 164-168.
García, I. E., Maripillán, J., Jara, O., Ceriani, R., Palacios-Muñoz, A., Ramachandran, J., Olivero, P., Perez-Acle, T., González, C., Sáez, J. C. et al. (2015). Keratitis-ichthyosis-deafness syndrome-associated Cx26 mutants produce nonfunctional gap junctions but hyperactive hemichannels when co-expressed with wild type Cx43. *J. Invest. Dermatol.* **135**, 1338-1347.
Jan, A. Y., Amin, S., Ratajczak, P., Richard, G. and Sybert, V. P. (2004). Genetic heterogeneity of KID syndrome: identification of a Cx30 gene (GJB6) mutation in a patient with KID syndrome and congenital atrichia. *J. Invest. Dermatol.* **122**, 1108-1113.
Johnson, S. L., Ceriani, F., Houston, O., Polishchuk, R., Polishchuk, E., Crispino, G., Zorzi, V., Mammano, F. and Marcotti, W. (2017). Connexin-mediated signaling in nonsensory cells is crucial for the development of sensory inner hair cells in the mouse cochlea. *J. Neurosci.* **37**, 258-268.
Kalinec, G. M., Park, C., Thein, P. and Kalinec, F. (2016). Working with auditory HEI-OC1 Cells. *J. Vis. Exp.* **115**, 54425.
Kelly, J. J., Simek, J. and Laird, D. W. (2015). Mechanisms linking connexin mutations to human diseases. *Cell Tissue Res.* **360**, 701-721.
Kenneson, A., Van Naarden Braun, K. and Boyle, C. (2002). GJB2 (connexin 26) variants and nonsyndromic sensorineural hearing loss: a HuGE review. *Genet. Med.* **4**, 258-274.
Kikuchi, T., Kimura, R. S., Paul, D. L. and Adams, J. C. (1995). Gap junctions in the rat cochlea: immunohistochemical and ultrastructural analysis. *Anat. Embryol.* **191**, 101-118.
Laird, D. W. (2006). Life cycle of connexins in health and disease. *Biochem. J.* **394**, 527-543.
Lamartine, J., Munhoz Essenfelder, G., Kibar, Z., Lanneluc, I., Callouet, E., Laoudj, D., Lemaître, G., Hand, C., Hayflick, S. J., Zonana, J. et al. (2000). Mutations in GJB6 cause hidrotic ectodermal dysplasia. *Nat. Genet.* **26**, 142-144.
Lautermann, J., ten Cate, W.-J. F., Altenhoff, P., Grümmer, R., Traub, O., Frank, H.-G., Jahnke, K. and Winterhager, E. (1998). Expression of the gap-junction connexins 26 and 30 in the rat cochlea. *Cell Tissue Res.* **294**, 415-420.
Lu, Y., Zhang, R., Wang, Z., Zhou, S., Song, Y., Chen, L., Chen, N., Liu, W., Ji, C., Wu, W. et al. (2018). Mechanistic effect of the human GJB6 gene and its mutations in HaCaT cell proliferation and apoptosis. *Brazilian J. Med. Biol. Res.* **51**, e7560.
Lukashkina, V. A., Levic, S., Lukashkin, A. N., Strenzke, N. and Russell, I. J. (2017). A connexin30 mutation rescues hearing and reveals roles for gap junctions in cochlear amplification and micromechanics. *Nat. Commun.* **8**, 14530.
Mahendrasingam, S., Macdonald, J. A. and Furness, D. N. (2011). Relative time course of degeneration of different cochlear structures in the CD/1 mouse model of accelerated aging. *J. Assoc. Res. Otolaryngol.* **12**, 437-453.
Mann, Z. F., Duchen, M. R. and Gale, J. E. (2009). Mitochondria modulate the spatio-temporal properties of intra- and intercellular Ca2+ signals in cochlear supporting cells. *Cell Calcium* **46**, 136-146.
Marcus, D. C., Wu, T., Wangemann, P. and Kofuji, P. (2002). KCNJ10 (Kir4.1) potassium channel knockout abolishes endocochlear potential. *Am. J. Physiol. Physiol.* **282**, C403-C407.
Mhaske, P. V., Levit, N. A., Li, L., Wang, H.-Z., Lee, J. R., Shuja, Z., Brink, P. R. and White, T. W. (2013). The human Cx26-D50A and Cx26-A88V mutations causing keratitis-ichthyosis-deafness syndrome display increased hemichannel activity. *Am. J. Physiol. Cell Physiol.* **304**, C1150.
Nagy, J. I., Patel, D., Ochalski, P. A. Y. and Stelmack, G. L. (1999). Connexin30 in rodent, cat and human brain: selective expression in gray matter astrocytes, co-localization with connexin43 at gap junctions and late developmental appearance. *Neuroscience* **88**, 447-468.
Neijssen, J., Herberts, C., Drijfhout, J. W., Reits, E., Janssen, L. and Neefjes, J. (2005). Cross-presentation by intercellular peptide transfer through gap junctions. *Nature* **434**, 83-88.
Nin, F., Hibino, H., Doi, K., Suzuki, T., Hisa, Y. and Kurachi, Y. (2008). The endocochlear potential depends on two K+ diffusion potentials and an electrical barrier in the stria vascularis of the inner ear. *Proc. Natl. Acad. Sci. USA* **105**, 1751-1756.
Ortolano, S., Di Pasquale, G., Crispino, G., Anselmi, F., Mammano, F. and Chiorini, J. A. (2008). Coordinated control of connexin 26 and connexin 30 at the regulatory and functional level in the inner ear. *Proc. Natl. Acad. Sci. USA* **105**, 18776-18781.
Oxenham, A. J. and Bacon, S. P. (2003). Cochlear compression: perceptual measures and implications for normal and impaired hearing. *Ear Hear.* **24**, 352-366.
Retamal, M. A., Reyes, E. P., García, I. E., Pinto, B., Martínez, A. D. and González, C. (2015). Diseases associated with leaky hemichannels. *Front. Cell. Neurosci.* **9**, 267.
Sáez, J. C. and Leybaert, L. (2014). Hunting for connexin hemichannels. *FEBS Lett.* **588**, 1205-1211.
Schütz, M., Scimemi, P., Majumder, P., De Siati, R. D., Crispino, G., Rodriguez, L., Bortolozzi, M., Santarelli, R., Seydel, A., Sonntag, S. et al. (2010). The human deafness-associated connexin 30 T5M mutation causes mild hearing loss and reduces biochemical coupling among cochlear non-sensory cells in knock-in mice. *Hum. Mol. Genet.* **19**, 4759-4773.
Schutz, M., Auth, T., Gehrt, A., Bosen, F., Korber, I., Strenzke, N., Moser, T. and Willecke, K. (2011). The connexin26 S17F mouse mutant represents a model for the human hereditary keratitis-ichthyosis-deafness syndrome. *Hum. Mol. Genet.* **20**, 28-39.
Smith, F. J. D., Irwin McLean, W. H. and Morley, S. M. (2002). A novel Connexin 30 mutation in Clouston syndrome. *J. Invest. Dermatol.* **118**, 530-532.
Snoeckx, R. L., Huygen, P. L. M., Feldmann, D., Marlin, S., Denoyelle, F., Waligora, J., Mueller-Malesinska, M., Pollak, A., Ploski, R., Murgia, A. et al. (2005). GJB2 mutations and degree of hearing loss: a multicenter study. *Am. J. Hum. Genet.* **77**, 945-957.
Sugiura, K., Teranishi, M., Matsumoto, Y. and Akiyama, M. (2013). Clouston syndrome with heterozygous GJB6 mutation p.Ala88Val and GJB2 variant p.Val27Ile revealing mild sensorineural hearing loss and photophobia. *JAMA Dermatol.* **149**, 1350-1351.
Sun, J., Ahmad, S., Chen, S., Tang, W., Zhang, Y., Chen, P. and Lin, X. (2005). Cochlear gap junctions coassembled from Cx26 and 30 show faster intercellular Ca^{2+} signaling than homomeric counterparts. *Am. J. Physiol. Physiol.* **288**, C613-C623.
Teubner, B., Michel, V., Pesch, J., Lautermann, J., Cohen-Salmon, M., Söhl, G., Jahnke, K., Winterhager, E., Herberhold, C., Hardelin, J.-P. et al. (2003). Connexin30 (Gjb6)-deficiency causes severe hearing impairment and lack of endocochlear potential. *Hum. Mol. Genet.* **12**, 13-21.
Xu, J. and Nicholson, B. J. (2013). The role of connexins in ear and skin physiology - functional insights from disease-associated mutations. *Biochim. Biophys. Acta* **1828**, 167-178.
Zhang, X.-J., Chen, J.-J., Yang, S., Cui, Y., Xiong, X.-Y., He, P.-P., Dong, P.-L., Xu, S.-J., Li, Y.-B., Zhou, Q. et al. (2003). A mutation in the connexin 30 gene in Chinese Han patients with hidrotic ectodermal dysplasia. *J. Dermatol. Sci.* **32**, 11-17.
Zhang, Y., Tang, W., Ahmad, S., Sipp, J. A., Chen, P. and Lin, X. (2005). Gap junction-mediated intercellular biochemical coupling in cochlear supporting cells is required for normal cochlear functions. *Proc. Natl. Acad. Sci. USA* **102**, 15201-15206.

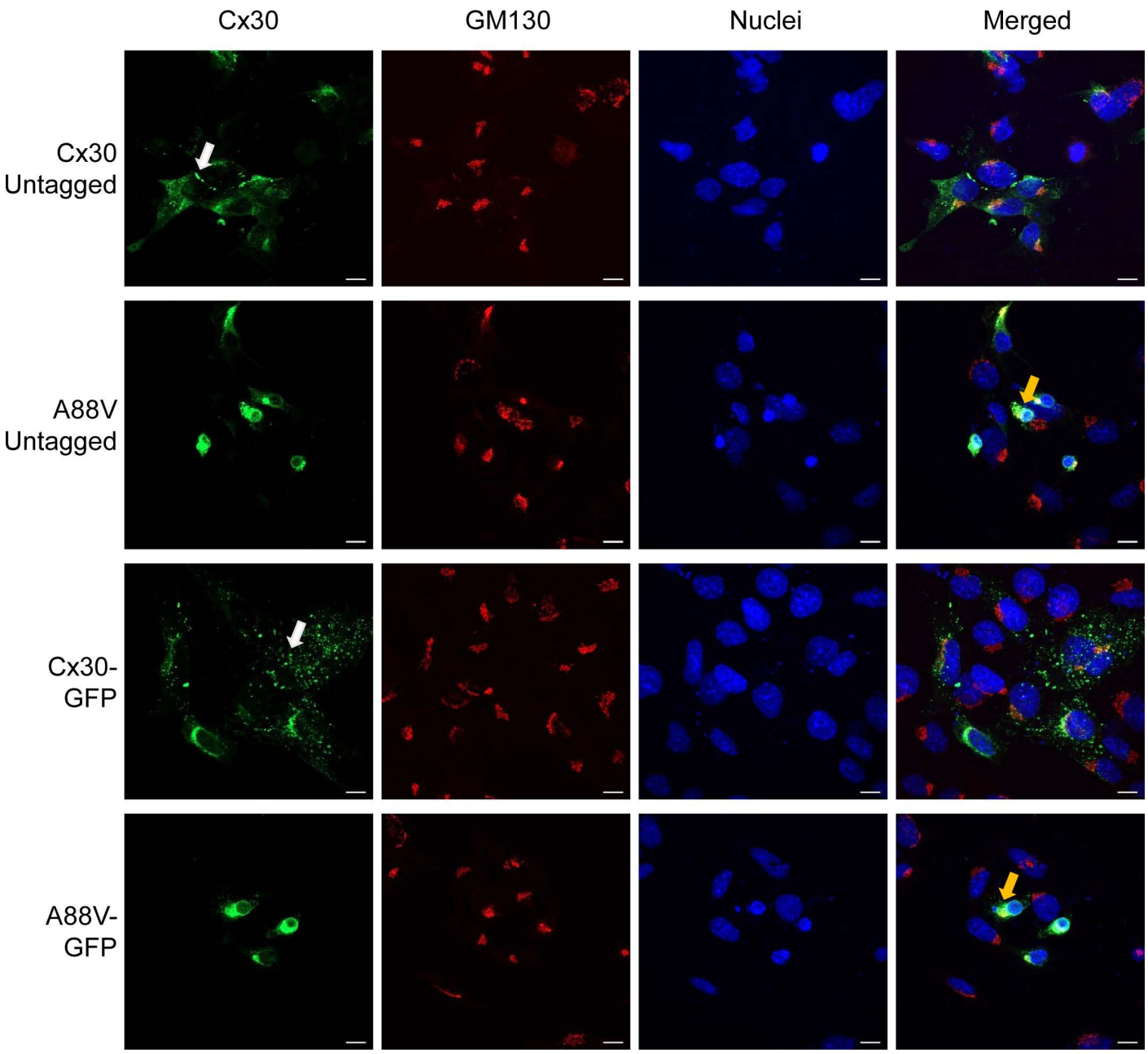

Figure S1. The A88V mutant partially localizes to the Golgi apparatus in surviving HEI-OC1 cells. HEI-OC1 cells were engineered to transiently express untagged or GFP-tagged wild-type Cx30 or the A88V mutant (green). Cells were immunostained for Cx30 (untagged, green) and the Golgi marker GM130 (red) and counterstained with Hoechst 33342 (blue) to label nuclei. In comparison to wild-type Cx30 and Cx30-GFP (white arrows), the A88V and A88V-GFP expressing cells exhibited a lack of gap junction-like puncta and partially co-localized with GM130 (orange arrows) in surviving cells. Bars, 10 µm.

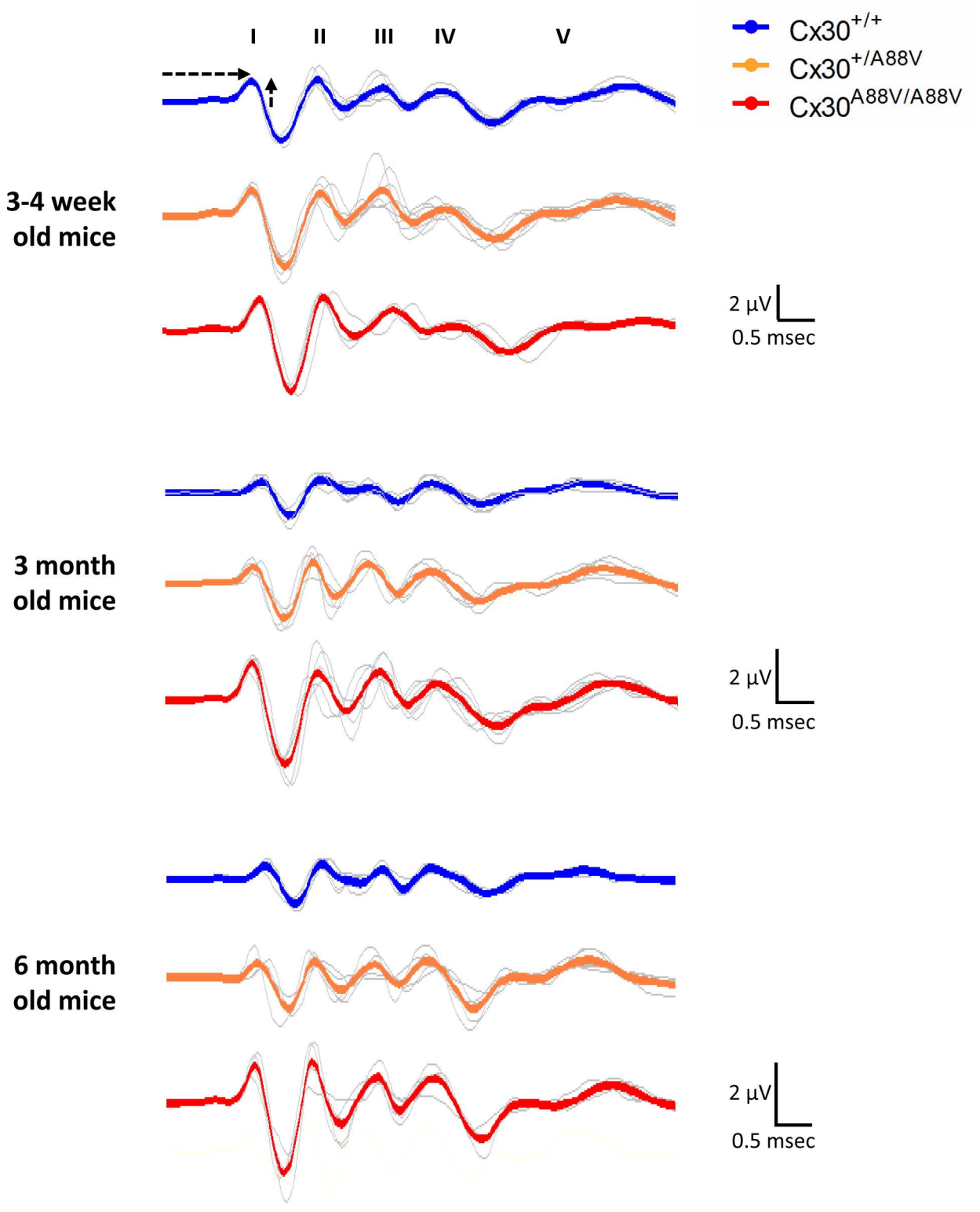

Figure S2. Average ABR traces for all age groups and across genotypes. ABR traces from the 90 dB-SPL click stimulus are shown overlaid (grey lines) and averaged (thick, coloured lines) for each genotype and age set. Amplitudes (in µV) were calculated from the peak of wave I and latencies (in msec) calculated as the time from stimulus onset to the peak of wave I, as indicated by the dashed arrows in the top panel. The traces show faster latencies and higher amplitudes for the homozygous A88V mutant mice compared to wild-type and heterozygous controls.